

Modelling of high quality pasta drying: mathematical model and validation

Massimo Migliori ^a, Domenico Gabriele ^a, Bruno de Cindio ^{a,*}, Claudio M. Pollini ^b

^a *Laboratory of Rheology, Department of Chemical Engineering and Materials, University of Calabria, Via P. Bucci Cubo 44/a, I-87030 Arcavacata di Rende (CS), Italy*

^b *Pavan S.p.A., via Monte Grappa 8, I-35015 Galliera Veneta (PD), Italy*

Received 10 November 2003; accepted 13 August 2004

Available online 18 October 2004

Abstract

The pasta drying process was studied using an engineering approach. The phenomena of mass and heat exchange between pasta samples and air was modelled according to the classic transport approach applied to a hollow cylindrical shape pasta. Data from the literature and from measurements were used to fix the material parameter values of both the air and dough phases. Theoretical correlations were used to obtain a good estimate of mass and heat exchange coefficients between dough samples and air. The proposed model was set by choosing the mass transfer coefficient as the unique optimisation parameter, determined by best fitting of the experimental water content data obtained under given conditions in a static dryer. The model was then validated at different temperature and air humidity drying profiles and a good agreement with the experimental results was found. Finally the model was applied to different process conditions and the drying time was calculated from the simulations.

© 2004 Elsevier Ltd. All rights reserved.

Keywords: Drying; Food processing; Heat transfer; Mass transfer; Modelling; Pasta production

1. Introduction

In the last 10 years, owing to an increased market demand for dry pasta in many countries, the requirements of both product quality and production rate have increased too. These two aspects are very often considered in contrast each to the other because it is thought that high production rates, characterized by somehow severe process conditions, induce thermal and mechanical damages into the products. These aspects may strongly decrease pasta quality as evidenced by nutrient loss, bad colour, poor texture, marked consistency loss when

overcooking, etc. Of course only a careful control of the process conditions coupled to a deep knowledge of the material properties, may avoid those undesired effects, while still maintaining high production rates. Nevertheless, the production process is currently carried out in a rather empirical way, because it is still based on the practical knowledge of pasta-makers, instead of standing on very well consolidated process engineering basis. In fact, the choice of raw materials and process conditions is made by following “rules of thumb” that do not allow any control on the product quality, and they do not match high production rates.

Starting from this point, it clearly appears that an engineering approach has to be developed establishing the influence of the main process variables on the final product quality, in order to apply an effective production control. This objective may be achieved by making a global model capable of simulating what happens

* Corresponding author. Tel.: +39 984 496708/496687; fax: +39 984 496655.

E-mail addresses: migliori@unical.it (M. Migliori), d.gabriele@unical.it (D. Gabriele), bruno.decindio@unical.it (B. de Cindio), tecnologie@pavan.com (C.M. Pollini).

Nomenclature

a_w	water activity coefficient, –		
b	gradient pulse of strength in NMR measurements		
C	heat capacity, $\text{J kg}^{-1} \text{K}^{-1}$		
C_p	specific heat, $\text{J kg}^{-1} \text{K}^{-1}$		
D	water diffusivity, $\text{m}^2 \text{s}^{-1}$		
E_a	activation energy, kJ mol^{-1}		
F	echo attenuation in NMR measurements		
h	global heat exchange coefficient, $\text{J m}^{-2} \text{K}^{-1}$		
I	signal intensity in NMR measurements		
J_h	Colburn factor for heat transfer, –		
J_m	Colburn factor for mass transfer, –		
k	thermal conductivity, $\text{W m}^{-1} \text{K}^{-1}$		
k_x	global mass exchange coefficient, $\text{kg m}^{-2} \text{s}^{-1}$		
L	pasta sample length, m		
M	molecular weight, dalton		
N	mass flux, $\text{kg m}^{-2} \text{s}^{-1}$		
P	pressure, Pa		
p°	vapour pressure, Pa		
q	thermal flux, $\text{W m}^{-2} \text{K}^{-1}$		
R	sample radius, m		
r	variable radius, m		
R_g	universal gas constant, $\text{J g mol}^{-1} \text{K}^{-1}$		
SQM	square quadratic deviation, %		
T_∞	air temperature in bulk phase, K		
T	temperature, K		
t	time, s		
U	dough water content on wet basis, w/w		
UR_∞	relative water content of air in bulk phase, w/w%		
v_∞	air velocity, m s^{-1}		
x	dough water content on dry basis, –		
y	molar fraction in air, –		
$y_{w,\infty}$	water molar fraction in air in bulk phase, –		
		<i>Dimensionless numbers</i>	
		Nu	Nusselt
		Pr	Prandtl
		Re	Reynolds
		Sc	Schmidt
		Sh	Sherwood
		<i>Greek symbols</i>	
		Δ	space variation
		α	shrinkage coefficient, –
		δ	pasta sample thickness, mm
		β	theoretical and optimised mass exchange coefficient ratio, –
		λ	water latent heat of vaporization, J kg^{-1}
		ρ	dough density, kg m^{-3}
		σ	time between 90° and 180° rf in NMR measurements
		ψ	duration of the gradient pulse in NMR measurements
		ζ	magnetogyric ratio in NMR measurements
		<i>Subscripts</i>	
		0	initial condition
		a	air
		d	dough
		exp	experimental value
		f	film condition
		i	generic point of calculation grid
		sim	simulation value
		w	water
		<i>Superscripts</i>	
		eq	equilibrium conditions
		ext	referred to external surface
		int	referred to internal surface

during the process and therefore to predict “a priori” the values of the desired properties.

In this work attention was focused on the study and modelling of the pasta drying process, because during this step pasta is subjected to rather severe conditions that are fully responsible for the final product quality. In fact, drying is usually realised by using wet hot air with temperatures ranging between 80 and 120°C, and a controlled relative humidity UR ranging between 40% and 70%. The actual industrial trend is to get rather high production rates over 3–4000 kg/h, that are obtained by reducing the drying time by means of a process characterised by high temperature and low moisture drying air, this choice in turn reduces the microbiological risk because of the strong heat treatment. Moreover, according to the market request for

high quality production, these severe process conditions may cause a so-called “thermal damage” that is evidenced by a poor texture, a decrease in the mechanical resistance, a lower nutrient content, a darker colour, etc. This kind of product obviously does not fit with consumer expectations, even if safer from a microbiological point of view, owing to the poorness of most of the quality indices.

Dried pasta production process can be represented schematically as a rather simple chain of unit operations (see Fig. 1). Ingredients, basically water and durum wheat flour, are usually mixed together under vacuum to give a dough with a water content percentage close to 30% (wet basis). Then the resulting dough is sent into an extruder press and finally extruded through a head in order to obtain the desired pasta shape.

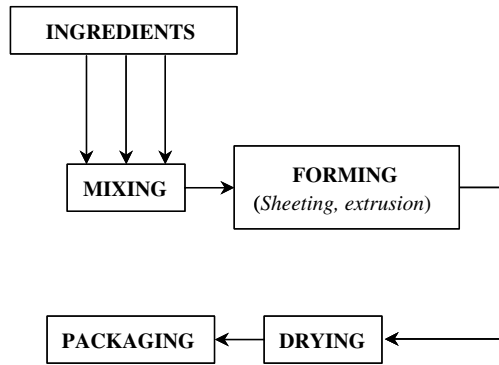


Fig. 1. Pasta production process flow sheet.

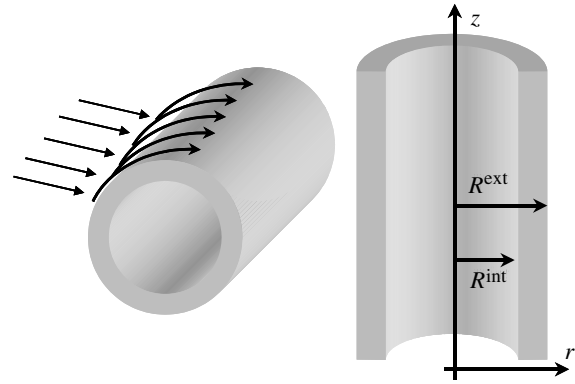


Fig. 2. Geometrical scheme of pasta sample.

The drying process is afterward carried out by exploiting the humidity and temperature difference between samples and air, causing the water content to decrease inside the sample. Thus the applied external drying air temperature and humidity must be related to the pasta properties as a function of time, to determine the optimal process conditions according to any given pasta quality criterion. Therefore the aim of the present work is to make available a predictive model that gives the water loss occurring inside the pasta as resulting from the applied external conditions during drying, allowing one to know “a priori” the resulting transient water content profile inside the pasta. It should be noted that drying of pasta requires several hours, therefore any predictive model capable of predicting transient water content is welcome, allowing a strong reduction of expensive trials needed to find the best operational conditions.

2. Mathematical modelling

The drying process of “short pasta” was modelled using hollow cylindrical shaped pasta that was simplified as a cylindrical shell with an infinite length. Because of the small value of the ratio δ/L , border effects can be neglected. In addition, the external surface of the sample was supposed to be surrounded by hot moist air with controlled properties (i.e., temperature T_∞ and relative humidity UR_∞). Owing to the considered geometrical shape, an azimuthal symmetry holds, and therefore only r -direction variations were considered (Fig. 2). Consequently, the heat transfer balance equations is written as (Bird, Stewart, & Lightfoot, 1960):

$$\rho_d \cdot C_d \cdot \frac{\partial T}{\partial t} = \frac{1}{r} \cdot \frac{\partial}{\partial r} \left[r \cdot k_d \cdot \frac{\partial T}{\partial r} \right] \quad (1)$$

where the thermal conductivity (k_d) and heat capacity (C_d) are assumed to be both temperature and water content dependent. The dough density (ρ_d) has been assumed as a constant because in a previous work (de

Cindio, Brancato, & Saggese, 1992) it was shown that ρ_d does not reasonably depend on temperature and, in addition, even a weak dependence on water content was observed. According to that the following final form may be obtained for the mass-transfer equation if Fick’s diffusion law is used to describe the water transport inside the dough:

$$\frac{\partial U}{\partial t} = \frac{1}{r} \cdot \frac{\partial}{\partial r} \left[r \cdot D_d \cdot \frac{\partial U}{\partial r} \right] \quad (2)$$

In Eq. (2) U is the water content inside the dough expressed on a wet basis (w.b.), i.e., the ratio of water weight and total weight, and water diffusivity (D_d) depends on temperature and water content. Moreover, the general statement of assuming all the material parameters as a function of T and U , leads to a system of linked differential equations that was solved according to well-determined boundary conditions for both external and internal surfaces.

2.1. Boundary conditions

The solution of the differential equation system (Eqs. (1) and (2)) needs two boundary conditions and one initial condition both for mass and energy transports. The main hypothesis is the thermodynamic equilibrium condition at the air–dough interface (Fig. 3) that, in turn, is

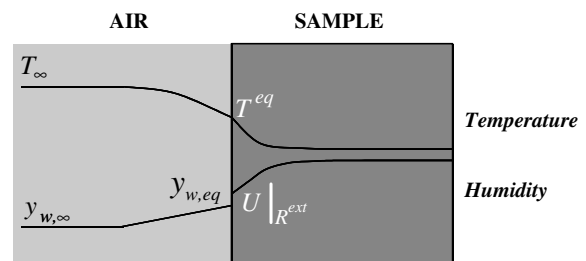


Fig. 3. Air–dough interface scheme.

also assumed to coincide with the evaporation front. This implies that the air and dough interface chemical potentials must be equal. By writing this latter in terms of water-activity it follows:

$$Py_w^{\text{eq}} = p_w^{\circ} a_w \quad (3)$$

where P is the pressure of the system, y_w^{eq} the water molar fraction in air at equilibrium conditions, p_w° the vapour pressure and a_w the water activity. In Eq. (3) the vapour phase is assumed to behave as an ideal gas solution, while the liquid phase is considered as a real mixture, deviating from the Raoult solution chosen as the reference state. Then the value of a_w may be expressed by any constitutive equation relating water activity to the dough water content U .

The mass boundary condition stands on the continuity of the mass flux at the air–dough interfaces, that at the external surface reads:

$$-\rho_d D_d \left. \frac{\partial U}{\partial r} \right|_{R^{\text{ext}}} = N_w^{\text{ext}} = k_x^{\text{ext}} M_w (y_{w,\infty} - y_w|_{R^{\text{ext}}}) \quad (4)$$

where the water mass flux N_w^{ext} on the air side has been written in terms of a global transport coefficient k_x^{ext} , whilst the mass transfer mechanism inside the dough has been assumed to be diffusive. In Eq. (4), M_w stands for water molecular weight and y_{∞} and $y_w|_{R^{\text{ext}}}$ for water molar fraction of the drying air bulk and the air–dough interface respectively. Of course, according to the assumed equilibrium conditions at the interface, it follows that:

$$y_w^{\text{eq}} = y_w|_{R^{\text{ext}}} \quad (5)$$

Concerning the heat transfer at the external interface, owing to the equilibrium assumption at the interface air–dough, the surface temperature corresponds to the equilibrium temperature T^{eq}

$$T^{\text{eq}} = T|_{R^{\text{ext}}} \quad (6)$$

At the air–dough interface the continuity of heat flux holds and may be written as:

$$\lambda N_w^{\text{ext}} - k_d \left. \frac{\partial T}{\partial r} \right|_{R^{\text{ext}}} = q_a^{\text{ext}} = h^{\text{ext}} \cdot (T_{\infty} - T|_{R^{\text{ext}}}) \quad (7)$$

where λ is the water molar latent heat of evaporation. The air-side thermal flux q_a^{ext} has been written using a global exchange coefficient h^{ext} , and the flux inside the dough at the interface is expressed as the sum of two terms: the first one is due to water evaporation while the second one to the heat conduction.

It should be noticed that during simultaneous mass and heat transport, when it is possible to assume that water diffusion inside the dough is fast enough to transport a sufficient amount of water to the evaporating surface, the system behaves like a wet bulb thermometer (Bird et al., 1960). This means that the heat supplied by the drying air is just equal to the heat absorbed as

a consequence of the evaporation. Thus in this case Eq. (7) becomes:

$$q_a^{\text{ext}} = \lambda N_w^{\text{ext}} \quad (8)$$

This phenomenon leads to a constant temperature value determined as a function of the equilibrium condition expressed by Eq. (3) and known as the “wet bulb temperature”. It should be noticed that temperature does not rise until this condition holds, i.e., until the amount of water transported to the evaporating surface is capable of compensating the drying air heat supply. Drying further, the evaporation becomes insufficient and therefore the surface temperature starts to rise, and consequently a temperature gradient is found inside the dough.

The use of the global exchange coefficient h^{ext} and k_x^{ext} both for heat and mass transport at the external surface, allows the fluxes to be related directly to the temperature and the water molar fraction difference between air and sample (Bird et al., 1960). By taking into account the equilibrium, according to Eqs. (5) and (6), the two boundary conditions expressed by Eqs. (4) and (7) may be combined to obtain the following expression at the external surface:

$$h^{\text{ext}} \cdot (T_{\infty} - T^{\text{eq}}) = \lambda \cdot k_x^{\text{ext}} \cdot M_w \cdot (y_{w,\infty} - y_w^{\text{eq}}) + k_d \left. \frac{\partial T}{\partial r} \right|_{R^{\text{ext}}} \quad (9)$$

The second boundary condition for both heat and mass transport must be referred to the internal surface. It should be noticed that the transport phenomena occurring in the hollow of the cylinder is rather difficult to model because the air velocity is very low, and therefore the classic transfer coefficients should not apply. The mass transfer mechanism was divided into two steps: a radial-axial diffusion of water from the internal surface up to the sample edge, and the water removal by the air stream that grazes the sample. If the diffusive step prevails, the exchange mechanism may be modelled as the pure diffusive transport in a stagnant fluid (Bird et al., 1960), and the corresponding expressions for both heat and mass transfer may be applied. The use of this rigorous approach is rather complex, whereas the contribution to the total water removal is rather small; therefore, for the sake of simplicity, the transport steps have been grouped using again an overall exchange coefficient analogous to that introduced by Eq. (4). For the calculation of k_x^{int} and h^{int} the same method used for the external transport was applied but the air velocity was simply assumed to be three orders of magnitude less than the external velocity. In this way, the evidence that the internal surface was not directly exposed to the air flux was approximately taken into account.

The initial conditions assume constant uniform values of both temperature (T_0) and water content (U_0) throughout the sample.

2.2. Transport coefficients

The global heat transfer coefficient h^{ext} was calculated by means of the Colburn factor J_h (Bird et al., 1960) defined in terms of dimensionless numbers as

$$J_h = NuRe^{-1}Pr^{-1/3} \quad (10)$$

where Re is the Reynolds number, $Nu = h_a(2 \cdot R^{\text{ext}})/k_a$ is the Nusselt number and $Pr = \mu_a c p_a / k_a$ is the Prandtl number. By assuming a two-parameter model, the following correlation was used:

$$J_h = aRe^b \quad (11)$$

where a and b are material parameters the values of which for $Re > 100$ are (Sherwood & Pifgord, 1952)

$$a = 0.4096 \quad (12)$$

$$b = -0.4485 \quad (13)$$

For the determination of the mass transfer coefficient k_x , both for the external and internal surface, the classic Chilton–Colburn analogy (Bird et al., 1960), was used:

$$J_h = J_m \quad (14)$$

where J_m , is the mass Colburn coefficient defined as

$$J_m = ShRe^{-1}Sc^{-1} \quad (15)$$

$Sh = k_x(2 \cdot R^{\text{ext}})/D_a$ is the Sherwood number, $Sc = \nu_a/D_a$ is the Schmidt number. For cylindrical shell in psychrometry problems, k_x can be easily derived as (Bird et al., 1960):

$$k_x^{\text{ext}} = \frac{h^{\text{ext}}}{Cp_{a,f}} \cdot \left(\frac{Sc}{Pr}\right)^{2/3} \quad (16)$$

Obviously all the material parameters of the above quoted dimensionless numbers refer to the air–water system. The physical properties of wet air were evaluated at “film temperature” and at “film concentration”

$$T_f = \frac{T_\infty + T|_{R^{\text{ext}}}}{2} \quad (17)$$

$$y_{w,f} = \frac{y_{w,\infty} + y_w^{\text{ext}}}{2} \quad (18)$$

In the previous equation the mass diffusion coefficient D_a of water in air was calculated using the following literature correlation (Perry & Green, 1984):

$$D_a = \frac{10^{-3} \cdot T_f^{1.75} \left(\frac{M_a + M_w}{M_a \cdot M_w}\right)^{1/2}}{P \cdot \left[(\Sigma v)_a^{1/3} + (\Sigma v)_b^{1/3}\right]^2} \quad (19)$$

where P [atm] is the external pressure, M is the molecular weight of involved chemical species and (Σv) is a material parameter that depends on the atomic diffusion volumes. For air and water the following values of (Σv) are suggested (Perry & Green, 1984):

$$(\Sigma v)_a = 20.1 \quad (20)$$

$$(\Sigma v)_w = 12.7 \quad (21)$$

2.3. Shrinkage

During drying, dough is subjected to large changes because water content percentage decreases from 31% to 11.5% (w.b.), with the consequence of a marked reduction of the sample radius. This shrinkage was modelled according to a linear relationship between geometrical reduction and water content, (Lang, Sokhansanj, & Rohani, 1994; Minshkin, Saguy, & Karel, 1984):

$$R = R_0[1 + \alpha(U - U_0)] \quad (22)$$

This equation was originally proposed for a uniform water content internal profile, but during drying a water profile inside the pasta is usually expected, therefore the shrinkage must depend on radial position. According to that, a modified form of Eq. (22) was developed (Suarez & Viollaz, 1991), by assuming that water content is constant in any radial segment Δr_i . Thus the geometrical contraction was evaluated as follows in any segment between two adjacent points of the calculation grid:

$$\Delta r_i = \Delta r_0[1 + \alpha(U_i - U_{i,0})] \quad (23)$$

The α value was assumed 0.42 according to Andrieu, Gonnet, and Laurent (1989).

2.4. Solution method

The simulation program was written in Visual Basic language and Eqs. (1) and (2), coupled with boundary conditions (Eqs. (3)–(6), for both internal and external surface) and was numerically solved by using finite differences (Finlayson, 1980) according to a classical Crank–Nicholson method. This method requires in principle an equal spaced calculation grid that is obtained by dividing the radial coordinates in segments of the same length. However, due to the internal water content profile a differential shrinkage inside the sample is expected. This implies that the segments between three adjacent points do not have the same length (Fig. 4) and, therefore the classical Crank–Nicholson method, that requires equal radial spacing, cannot be used. This

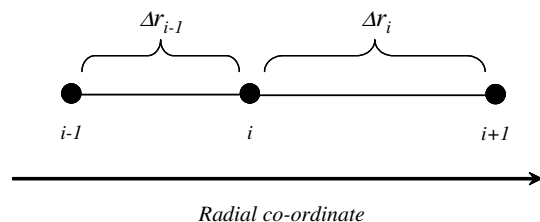


Fig. 4. Calculation grid.

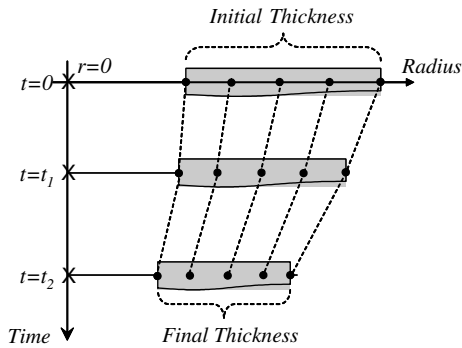


Fig. 5. Schematic representation of radius shrinkage.

difficulty was overcome by assuming at each grid point an equal radial interval Δr^* , obtained as the arithmetical average of two adjacent segments as follow:

$$\Delta r^* = \frac{\Delta r_i + \Delta r_{i+1}}{2} \quad (24)$$

With this assumption, the Crank–Nicholson method can still be applied. For example, the water content first derivative at any given i -point, may be calculated as:

$$\left. \frac{\partial U}{\partial r} \right|_i = \frac{U_{i+1} - U_{i-1}}{\Delta r^*} \quad (25)$$

The adopted method leads to a linear equation system that was solved by means of the classic Thomas's algorithm. In addition, according to the r -grid is time-dependency, the Δr_i value must be updated at each time using Eqs. (17)–(24), by considering either the water content or temperature profile calculated at the previous time step. In Fig. 5 a scheme of radius contraction during time is reported.

2.5. Simulation software

The solution method of the set of equation has been implemented in a computer program written in Visual Basic 6.0 language (Microsoft, USA). The prepared software allows numerically solving the balance equation, by means of non-accessible subroutines, whilst either material parameters or process conditions can be set by the user. The final simulation results, i.e., temperature and moisture content profiles, are available in a quick plot and may be converted and analysed by a normal calculation worksheet. In addition some other important technological parameters linked to the drying process such as shrinkage value and water activity may be easily obtained from the main results. The program has been organised in different frames grouping homologous properties and process parameters that can be changed, also using a small database, according to the simulative needs. This aspect does not have to be under-rated because the software may be easily run, during industrial production or research work, also from user

that are not get used to numerical calculation and modelling. Finally, the effort dedicated to make the simulation program friendly represents an important “follow up” of the present study because the software may be directly connected to the PLC controllers of the entire production cycle supplying predictive data to the controller with a meaningful reduction of the response time of the control loop.

3. Materials and methods

3.1. Dough properties

Often it is rather difficult to have a good estimation of thermal and physical properties of food. In the open literature several general semi-empirical model have been proposed (Saravacos & Kostaropoulos, 1996), even though all the properties are strongly dependent on the considered food. Particularly concerning the dough system, a high level of uncertainty on the properties measurements is generally found, essentially due to both a water loss during measurement and a marked difference between raw materials. Therefore dough literature data are often very different each from the other (Rask, 1989). In fact, many correlations have been proposed to correlate dough thermal conductivity k_d to water content and temperature. In this work the following four parameters model was used (Saravacos & Maroulis, 2001):

$$k_d(x, T) = \frac{1}{1+x} \lambda_0 \exp \left[-\frac{E_0}{R} \left(\frac{1}{T} - \frac{1}{T_{\text{Rif}}} \right) \right] + \frac{x}{1+x} \lambda_i \exp \left[-\frac{E_i}{R} \left(\frac{1}{T} - \frac{1}{T_{\text{Rif}}} \right) \right] \quad (26)$$

where x is the dough water content on dry basis, λ_i , λ_0 , E_i , E_0 are dough material parameters (Table 1), T [°C] is the dough temperature and T_{Rif} [°C] is a reference temperature fixed at 60°C (Saravacos & Maroulis, 2001). For sake of simplicity, this model was used to obtain an average value of k_d in the range of temperature and water content used in the process. By considering that dough temperature ranges between 313 and 353 K and the relative humidity ranges between 30% and 10% (w.b.), using Eq. (26) the following value of k_d was obtained:

Table 1
Parameters for pasta thermal conductivity calculation (Saravacos and Maroulis, 2001)

λ_i [W m ⁻¹ K ⁻¹]	0.8
λ_0 [W m ⁻¹ K ⁻¹]	0.273
E_i [kJ mol ⁻¹]	2.7
E_0 [kJ mol ⁻¹]	0.0

$$k_d = 0.41 \left[\frac{W}{m \cdot K} \right] \quad (27)$$

The dough density was calculated as function of moisture (de Cindio et al., 1992):

$$\rho_d = \frac{1}{(3.02 \cdot U + 6.46) \times 10^{-4}} \left[\frac{\text{kg}}{\text{m}^3} \right] \quad (28)$$

The heat capacity C_d was computed as a weighed average of the heat capacities C_i of the dough main components, i.e., water, starch and gluten (Andrieu et al., 1989):

$$C_d = \sum_i C_i \cdot x_i \quad (29)$$

The following values were used for the specific heat of the single components (de Cindio et al., 1992):

Water

$$C_w = 4.184 \left[\frac{\text{J}}{\text{gK}} \right] \quad (30)$$

Starch

$$C_s = 5.737 \cdot T + 1328 \left[\frac{\text{J}}{\text{gK}} \right] \quad (31)$$

Gluten

$$C_g = 6.329 \cdot T + 1465 \left[\frac{\text{J}}{\text{gK}} \right] \quad (32)$$

Dough composition was obtained from data in Table 2.

Water diffusivity in dough was measured by the NMR technique by using a Bruker NMR Spectrometer (Bruker, USA), modified by Stelar (Milan, Italy) working at a protonant resonance frequency of 80 MHz.

The water diffusivity determination was carried out using PFGSE (Pulsed Field gradient Spin-Echo) 1H-NMR technique (Coppola, La Mesa, Ranieri, & Terenzi, 1993) with an usual pulse sequence consisting of a 90° radio frequency (rf) pulse at $t = 0$ followed by a 180° rf pulse at $t = \sigma$; this results in a spin-echo at $t = 2\sigma$. In addition to rf pulses, a pulsed magnetic field gradient is inserted on each side of the 180° rf pulse, causing the attenuation of echo intensities. The parameters associated with the rf and magnetic field gradient pulse sequence are shown in Fig. 6. Assuming a free Gaussian diffusion, the theoretical expression of echo

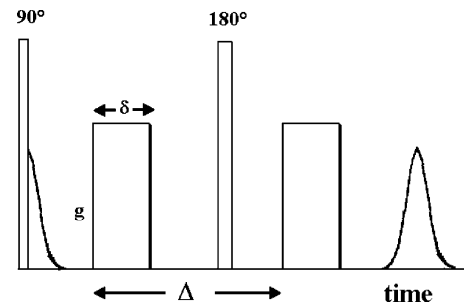


Fig. 6. Scheme of the magnetic field pulse sequence in NMR determination of water in dough diffusion.

attenuation F is given by the well-known Stejskal–Tanner equation (Coppola et al., 1993)

$$F = \frac{I(b)}{I(0)} = \exp \left[-(\zeta \psi b)^2 D_d \left(Q - \frac{\psi}{3} \right) \right] \quad (33)$$

where τ is the time between 90° and 180° rf pulses, $I(g)$ and $I(0)$ are the signal intensities at $t = 2\sigma$ in presence of gradient pulses of strength b and in the absence of any gradient pulses, respectively, ζ is the magnetogyric ratio, ψ is the duration of the gradient pulses, Θ is the time between the leading edges of the gradient pulses (time of the diffusion) and D_d is the water in dough diffusion.

The 90° rf pulse length was 9 μs, Θ and b were held constant to 0.020 s and 0.50 T/m, respectively.

The length of the gradient field pulse ψ was changed in the interval 0.001–0.006 s while the gradient strength b was calibrated using a reference sample of pure tri-distilled water, with a known self-diffusion coefficient. During the measurement, the gradient pulses direction was along the concentration and therefore the water in dough diffusion was detected.

The echo amplitude was measured accumulating 32 scans. The temperature was controlled by airflow regulation with a stability of ±0.2 °C.

The results obtained for samples of vacuumed dough with water content ranging between 33% and 22% (w.b.) are reported in Table 3. It was not possible to perform measurements on samples with a water content below 20%, because the signal was difficult to detect either for the low intensity or the fast relaxation time due to the bound water in the sample. Therefore for moisture

Table 2
Semolina flour composition

Water	14.78%
Protein	13.44%
Ash	0.87%
Wet Gluten	34.97%
Gluten	11.71%
Starch	24.23%

Table 3
Experimental water in dough diffusivity

Dough water content, w/w%	Water diffusivity, cm ² s ⁻¹
33	2.29 × 10 ⁻⁵
30	1.37 × 10 ⁻⁵
27	3.17 × 10 ⁻⁶
24	2.68 × 10 ⁻⁶
22	2.02 × 10 ⁻⁶

content below 22% the following semi-empirical model was applied (Waananen & Okos, 1996):

$$D_w = \left(1.2 \times 10^{-7} + \varepsilon \cdot \frac{8 \cdot 10^{-5}}{P} \right) \cdot \exp \left(-\frac{6.6e^{-20x} + E_a}{R_g T} \right) \quad (34)$$

where D_d is the water diffusivity in dough [m^2s^{-1}], P is the pressure [kPa], x the water weight fraction on dry basis (d.b.), i.e., the ratio of water weight and weight of dry components, T is the temperature [K], E_a the activation energy, that was found to be equal to $22.6 \text{ kJ gmol}^{-1}$ (Waananen & Okos, 1996), R gas universal constant and finally ε the pasta porosity, that was assumed as 0.26 (Xiong, Narsimman, & Okos, 1991). By combining measurements and correlations, water diffusivity D_d was obtained as a moisture multi-step function as shown in Fig. 7.

The water liquid–vapour equilibrium was modelled according to the classic Oswin constitutive equation (Schuchmann, Roy, & Peleg, 1990) that relates the water activity to water content:

$$a_w = \frac{\left(\frac{x}{a''}\right)^{1/b''}}{1 + \left(\frac{x}{a''}\right)^{1/b''}} \quad (35)$$

where a'' and b'' are model parameters containing the temperature dependence. The following values were used according to Andrieu, Stamatopoulos, and Zafirooulos (1985):

$$a = 0.154 - 1.22 \times 10^{-3} \cdot T \quad (36)$$

$$b = 7.8 \times 10^{-2} - 7.32 \times 10^{-3} \cdot T \quad (37)$$

where T is expressed as Kelvin degrees. Because the proposed model is valid when the water activity is higher than 0.5, it was first checked to ensure that this limit was not exceeded during drying. The water content range of interest is between 30% and 10%, corresponding to a_w values varying between 0.96 and 0.81, which are always within the validity range of Eq. (35).

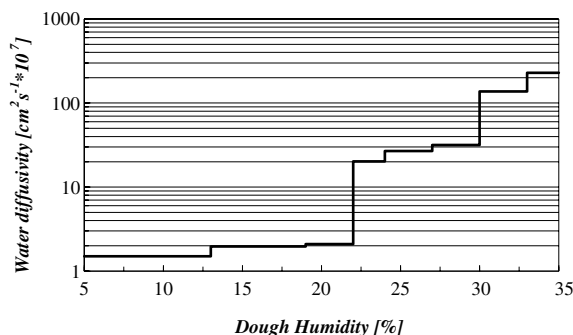


Fig. 7. Multi-step function of water diffusivity in dough.

3.2. Drying tests

The proposed model was tested experimentally by carrying out several drying tests under controlled conditions by means of a pilot static dryer (Pavan S.p.A., Italy), equipped with devices capable of giving the average temperature and water content of the samples during the treatment.

Pasta samples were prepared adding 27.5% (of the flour weight) of water to an industrial semolina flour (Jolly Sgambaro Godego, Italy) the composition of which is reported in Table 2. Samples were prepared using an integrated machine (Mod. PA1, Pavan S.p.A., Italy) consisting of a vacuum mixer, a compression screw and a head-cutter apparatus. Ten kilograms of semolina and 2.75 kg of water were mixed for 15 min and the resulting dough was shaped as hollow cylindrical samples, with a radius of 0.5 cm, a length of 3.5–5 cm and 1 mm thick. By taking into account the water percentage of the flour, as reported in Table 2, the final dough had a 0.325 w/w of moisture on a wet basis.

Several samples, about 12 kg per run, were loaded in the static drier (height 2 m, width 1.5 m, depth 1.5 m) laid down as a single layer on a series of trays. Drying was obtained by air circulation, and an electronic device controlled its humidity and temperature. During all the tests the temperature and humidity of the drying hot moist air was maintained at some fixed constant value. On the other hand, the air velocity was always the same by fixing the fan power. A direct measurement was done during the tests using an anemometer and a constant value of 0.5 m/s was found for all the runs.

Even though the drier was equipped with a weight cell to measure continuously the total water loss during the experiment, to get more accurate sample water content values, the average water content was obtained withdrawing five samples from the dryer every 10 min and measuring the weight by means of a thermo-balance (Sartorius, Germany). Every test was performed three times and the results obtained were statistically analysed by the “Few Sample Theory” (Kreyszig, 1970).

4. Model setting and validation

To verify the model reliability and check its sensitivity to process parameter changes, the proposed model was tested at different values of the main process variables temperature and humidity, following the experimental program reported in Table 4. The results were then compared to the simulation results coming out from the mathematical model set with the geometrical characteristics and initial conditions reported in Table 5. These conditions have been assumed to be constant for all the simulation performed for this validation work.

Table 4
Experimental plan for set and validation of the model

Treatment type	T_{∞} [K]	UR_{∞} [%]	v_{∞} [m s^{-1}]
Verify	353	68	0.5
Validation 1	353	58	0.5
Validation 2	343	58	0.5

Table 5
Initial condition and geometrical characteristics in simulation

Length L [mm]	35
External diameter R^{ext} [mm]	9.4
Averaged thickness δ [mm]	10
Initial moisture U [%]	30
Initial temperature T_0 [K]	303

A first experimental test was done in order to verify the model validity by applying usual operating conditions $T_{\infty} = 353\text{ K}$ and $UR_{\infty} = 68\%$ as set points and maintaining an air velocity value fixed to $v_{\infty} = 0.5\text{ m s}^{-1}$; this last value has been maintained constant for all the performed tests. In addition, the simulation results were based on the physical properties and transport coefficient previously discussed. The comparison between experimental and computed average water content profiles is shown in Fig. 8. It clearly shows that the transport coefficients computed with the proposed correlations, gave a simulated water content profile that largely exceeds the experimental one. This difference may be ascribed mainly to the empirical correlation used for computing the mass-transfer coefficient that assumes a single infinite cylinder dipped in an infinite mass of drying fluid. On the other hand, during the experimental drying process several samples were dispersed throughout the tray, and the amount of water extracted was affected by the particular pasta random orientation with respect to the air flux, even though the bed was maintained as a single layer. As a direct consequence, the mass flow was reduced with respect to the theoretical one and thus the simulated drying process was found to be much faster than the experimental process.

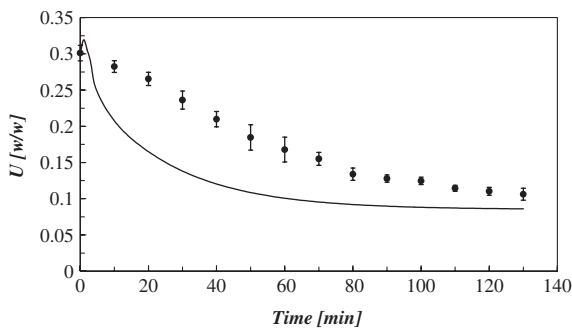


Fig. 8. Comparison between experimental and simulated data with theoretical correlations.

In order to overcome this problem, the mass flow needs to be reduced. Therefore an optimised mass-exchange coefficient k_x^{opt} was computed by considering the ratio β between k_x^{opt} and the calculated mass-exchange coefficient k_x as an adjustable parameter:

$$\beta = \frac{k_x^{\text{opt}}}{k_x} \tag{38}$$

The optimisation technique was performed using a classic goodness test method based on the minimization of the square quadratic deviation between experimental and computed average water content. Therefore a percentage deviation SQM was defined as

$$\text{SQM}\% = \sum_i \left(\frac{U_{\text{exp},i} - U_{\text{sim},i}}{U_{\text{exp},i}} \right)^2 \cdot 100 \tag{39}$$

where the sum is extended at any time to all the experimental water content points of the considered assessment drying test.

Different simulations were performed, with β ranging between 0.005 and 0.015, and the SQM% was calculated for each simulation referring to the considered experimental set up. The result is shown in Fig. 9, and a minimum value of $\text{SQM}\% = 0.63$ was found corresponding to $\beta = 0.0085$. Thus this value was chosen as the optimum of β and a new computation was performed with this value. As expected, a good agreement was found between the simulated and experimental curve (see Fig. 10), where a maximum error does not exceed 4%.

By the previous optimisation, the model was completely set and therefore it needed only to be validated to check its sensitivity to different process conditions as reported in Table 4. The first experimental trial was conducted by setting the air moisture to 58% and maintaining the air temperature at 353 K. From these new process conditions it was possible to check the model sensitivity to evaporation velocity changes. In fact, by lowering the air water content, the mass transfer driving force increases according to Eq. (4), and therefore dough water content should quickly decrease. The experimental and simulated data obtained for these process conditions are reported in Fig. 11. A rather

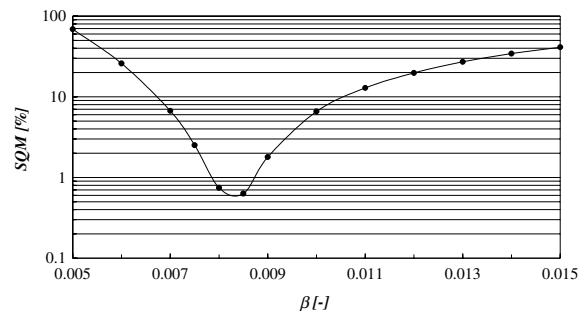


Fig. 9. β optimisation curve.

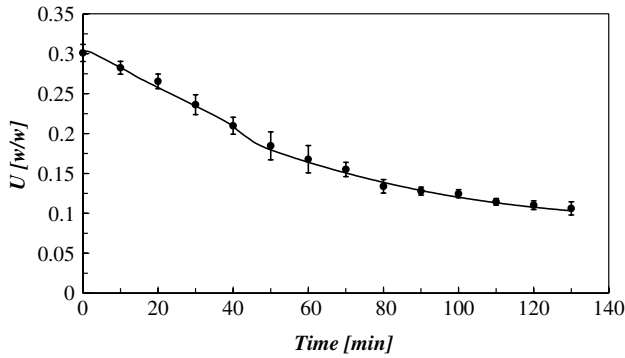


Fig. 10. Comparison between experimental and simulated data with optimised exchange coefficient ($T_{\infty} = 353$ K, $UR_{\infty} = 68\%$).

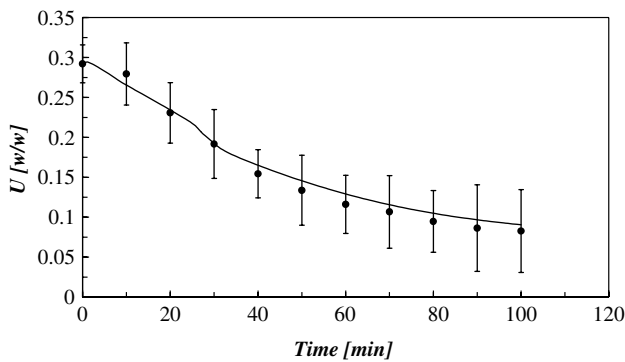


Fig. 11. Validation test at different temperature ($T_{\infty} = 353$ K, $UR_{\infty} = 58\%$).

good agreement was found with a maximum difference between the two curves of less than 12%.

To investigate the influence of temperature changes a test was done by setting temperature at 343 K and maintaining water content at 58%. It is expected that the reduction in temperature decreases the heat flux supplied to the sample and the process becomes slower. In Fig. 12 the comparison between experimental and simulated profiles is reported and again the agreement was rather good as confirmed by a maximum error that is

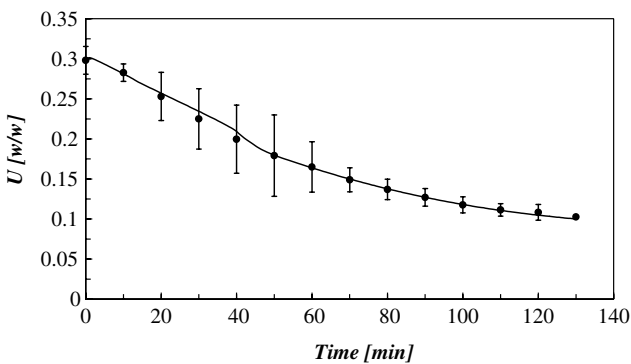


Fig. 12. Validation test at different air humidity ($T_{\infty} = 343$ K, $UR_{\infty} = 68\%$).

always below 5%. It clearly appears that the consideration outlined above has been confirmed by the experimental results.

5. Simulation tests and conclusions

In order to show how the proposed model can be helpful for industrial applications, in this section an example is proposed. The final water content can be obtained by following different temperature and water content paths during the process. In particular, the high temperature and low moisture value of the drying fluid tend to accelerate the drying process, while slow processes can be realised by using either low temperature or high humidity values. Depending on the adopted process conditions, the final water content value (fixed at 0.115 w/w) is reached at different “process time”, that can be easily computed by the simulative model when different drying conditions are applied, without making any expensive experimental test. Starting from the conditions reported in Table 4, simulations were performed applying the conditions reported in Table 6 that simulate extreme drying conditions. From the results plotted in Fig. 13, it clearly appears that the model gives large drying velocity differences, and as a consequence a wide range of process time values was determined and reported in Table 7.

Finally it should be noticed that, as shown above, the proposed simulative model avoids the rather expensive and time consuming trial error technique of process assessment, by drastically reducing the experimental tests to only those considered interesting by the produc-

Table 6
Process condition for simulation

Treatment type	T_{∞} [K]	UR_{∞} [%]	v_{∞} [m s^{-1}]
Strong	363	50	0.5
Mild 1	363	70	0.5
Mild 2	343	50	0.5
Soft	343	70	0.5

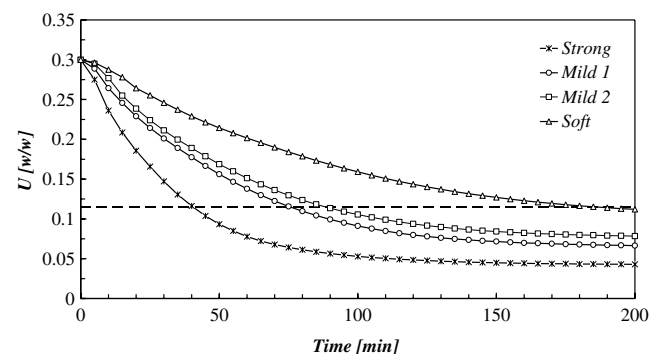


Fig. 13. “Process time” calculation: drying simulations.

Table 7
Calculated process time

Treatment type	Process time [min]
Strong	40
Mild 1	90
Mild 2	75
Soft	185

tion technologist. In addition, the simulative approach allows simplifies the experimental plan when a new product has to processed and different operating conditions need to be tested. Concerning this approach, it should be remarked that this is possible only using a simulative approach because the “expert systems” currently widely used, and based on some questionable numerical algorithms and not on physical models, and are rather stiff in the application.

In conclusion, this new engineering approach for dry pasta production can be considered as a starting point to model all the aspects of the process. In fact, the food quality represents the main new challenge for the manufacturer. The quality concept has to bring together many aspects such as nutritional control, microbiological safety and texture-flavour characteristics. As for pasta, starting from a model able to predict the moisture decrease during the process, all the quality parameters can be related to temperature and dough water content and a more accurate process might be realised. Moreover, this approach allows the manufacturers to strongly push the design of new products and processes, because the use of simulative tools opens new ideas without incurring the usual high research costs linked to pilot tests.

Acknowledgments

This work was developed in the frame of PNR TEMA 8 Industrial Research, granted by MURST that is acknowledged. The authors acknowledge Serena Avino for experimental tests and Francesco Carbone for his work, essential for the proposed software preparation. Dr. Cesare Oliverio is also grateful acknowledged for NMR measurements.

References

- Andrieu, J., Gonnet, E., & Laurent, M. (1989). Thermal conductivity and diffusivity of extruded durum wheat pasta. *Lebensmittel-Wissenschaft und Technologie*, 22, 6–10.
- Andrieu, J., Stamatopoulos, A., & Zafropoulos, M. (1985). Equation for fitting desorption isotherm of durum wheat pasta drying. *Journal of Food Technology*, 20, 651–657.
- Bird, R. B., Stewart, W. E., & Lightfoot, E. N. (1960). *Transport phenomena*. London (UK): John Wiley & sons.
- Coppola, L., La Mesa, C., Ranieri, G. A., & Terenzi, M. (1993). Analysis of water self-diffusion in polycrystalline lamellar systems by pulsed field gradient nuclear magnetic resonance experiments. *Journal of Chemical Physics*, 98, 5087–5090.
- de Cindio, B., Brancato, B., & Saggese, A. (1992). *Modellazione del processo di essiccamento di Paste Alimentari*. University of Naples, IMI-PAVAN Project—Final report.
- Finlayson, B. A. (1980). *Non-linear analysis in chemical engineering*. McGraw Hill Co.
- Kreyszig, E. (1970). *Introductory mathematical statistics*. John Wiley & Sons, Oxford University Press.
- Lang, W., Sokhansanj, S., & Rohani, S. (1994). Dynamic shrinkage and variable parameters in Bakker–Artema’s mathematical simulations of wheat and canola drying. *Drying Technology*, 13(8/9), 2181–2190.
- Minshkin, M., Saguy, I., & Karel, M. (1984). Optimization of nutrient retention during processing: ascorbic acid in potato dehydration. *Journal of Food Science*, 49, 1262–1266.
- Perry, R. H., & Green, D. (1984). *Perry’s Chemical Engineers’ Handbook* (6th ed.). New York (USA): McGraw-Hill.
- Rask, C. (1989). Thermal properties of dough and bakery products: A review of published data. *Journal of Food Engineering*, 9, 167–193.
- Saravacos, G. D., & Kostaropoulos, A. E. (1996). Engineering properties in food processing simulation. *Computers and Chemical Engineering*, 20, S461–S466.
- Saravacos, G. D., & Maroulis, Z. B. (2001). *Transport properties of food*. New York-Basel (USA): Marcel Dekker Inc.
- Schuchmann, H., Roy, I., & Peleg, M. (1990). Empirical models for moisture sorption isotherms at very high water activities. *Journal of Food Science*, 55, 759–762.
- Sherwood, T. K., & Pifgord, R. L. (1952). *Absorption and extraction* (2nd ed.). New York (USA): McGraw-Hill.
- Suarez, J. C., & Viollaz, P. E. (1991). Shrinkage effect on drying behaviour of potato slabs. *Journal of Food Engineering*, 13, 103–114.
- Waananen, K. M., & Okos, M. R. (1996). Effect of porosity on moisture diffusion during drying of pasta. *Journal of Food Engineering*, 28, 121–137.
- Xiong, X., Narsimhan, G., & Okos, M. R. (1991). Effect of composition and pore structure on binding energy and effective diffusivity of moisture in porous food. *Journal of Food Engineering*, 15, 189–208.